Design and Analysis of a Robust High Density Single Phase Isolated Buck Converter System For Regulated Power Supply

Amritansh Sagar
Department of Industrial Engineering
University of Padova
Padova, Italy
amritansh.sagar@studenti.unipd.it

Abhay Kumar
Department of Industrial Engineering
University of Padova
Padova, Italy
abhay.kumar@studenti.unipd.it

Manuele Bertoluzzo
Department of Industrial Engineering
University of Padova
Padova, Italy
manuele.bertoluzzo@unipd.it

***Abstract*— This paper proposes and delivers the performances and results of a simulated prototype of the single-phase isolated buck power converter system by extracting and transmitting the oscillating ripple energy of the primary buck inductor current to the secondary coil. This topology is an alteration on the conventional buck configuration in which the power inductor is changed with a coupled inductor to build an isolated secondary output. On inserting a coupled inductor in place of the power inductor of the buck converter, the secondary coil can deliver the required power due to the time-varying magnetic field developed by the oscillating part of the primary inductive current. Hence it eradicates the requirement of transmitter side in an inductively coupled power transfer technology and results in a DC-DC switching converter, including a primary coil besides the existing typical wired output of the buck converter. This paper addresses the relevant operating principle and offers results for the simulation prototype by using a single-phase isolated buck structure, which attains simultaneous Buck conversion of conventional output and delivers the power to the secondary load as well.**

Keywords*— *single-phase isolated buck power converter, regulated power supply, dc-dc converter, switching, charging

I. INTRODUCTION

Numerous applications like medical implants, portable electronics devices employ AC/DC [1-3] and DC/DC voltage regulators [4-5], ranging from very low power levels to 150 W or higher entail the use of multiple power tracks to deliver power to various devices inside a system. This is not rare for such power rails to just have varying load demands. To meet their separate power demand, a few rails may have to be quite closely controlled, with a minimal level of peak-to-peak difference. Some rails on the other hand, can deliver power that are more robust to variations on the input source and, hence, do not have these stringent regulations.

A traditional DC-DC power switching converter, like buck and boost converters, provides a controlled power, voltage and current to the load from a DC-source [6-7] via a wired link. The power inductor is an integral component of the converters that transmit a current involving a DC part along with an oscillating ripple part [7-8]. The time-varying magnetic field of the AC ripple creates a major problem with reference to electromagnetic interference (EMI) and conduction loss, however its capability to use as source for the isolated load is discussed in this work.

The Flyback topology [9-12] offers the possibility of producing multiple power lines from a single source, but that comes with a cost of using more complex control circuitry to regulate the secondary. The transformer [10-11]is the core of the flyback power source and undoubtedly the handiest aspect. Once implemented correctly, the transformer can provide the expected functionality while remaining economical. When improperly crafted, it can result in EMI problems, poor efficiency, and probable thermal overstress problems [12-13]. For designing the technology more user friendly and reducing the running cost of receiver side load like electric vehicle (EV), the uni-directional inductive wireless technology is replaced by bidirectional wireless power transfer system, to feed back the energy that store in EV battery pack, to another EVs, grid or home electrical instrument. [14-15]

This work proposes an approach for using this electromagnetic field caused by the AC ripple component that is associated with inductor current in the single-phase buck DC-DC switching converter, which is employed for the use of isolated secondary load as the regulated power input for the gate of the main MOSFET of the converter. The isolated power converter system attains DC-DC Buck operation (conventional power conversion) and isolated operation simultaneously that help to remove the requirement of setting up a separate DC/DC regulated supply for the main MOSFET. As a result, the entire system will be more efficient and cost-effective and also handle the same switching power circuit smoothly.

The following sections introduces the working concept of the envisaged model depending on the isolated buck converter structure. Section II describes the analysis and working of the proposed converter system. Section III describes the findings of the simulation model to validate the feasibility of the

proposed approach and concepts. The conclusion for the paper is specified in part IV.

II. ANALYSIS OF THE PROPOSED ISOLATED BUCK CONVERTER SYSTEM

This section discusses the idea and operating theory of the proposed power converter system, which simultaneously works as a DC-DC wired transmission and isolated operation. The basic principle of power inductor is by absorbing energy from the electrical circuit, and then stored this energy in a magnetic field and subsequently transferring this energy to the circuitry. In contrast to the real transformer, in which energy storage is undesirable, this approach employs a coupled inductor. The power MOSFET used here as high side switch of the converter is the commercial MOSFETS such as STL6N2VH5, STL66DN3LLH5. The secondary coil serves as the regulated power supply for the main switch of the converter. The simplistic circuit diagram of the single-phase isolated buck converter is depicted in Fig. 1. V_{in} represents the input for the system and V_{O1} and V_{O2} represent the two outputs of the system: one for typical wired buck power transfer and other for power transfer via coupled inductor. The secondary load depicted here has the same voltage and current rating as required by the above mentioned MOSFETS. The primary operating waveforms for the system are depicted in Fig. 2.

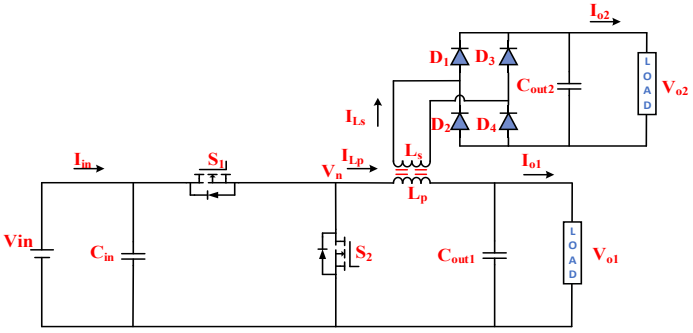

Fig. 1. Circuit Diagram of Single-Phase Isolated Buck system

The inductor magnetizing current I_m involves the primary side inductor current (I_{Lp}), the secondary side inductor current (I_{Ls}) and turns ratio of the coupled inductor ($\frac{N_2}{N_1}$) and it is expressed in equation (1). The primary side buck output voltage and secondary side output voltage is represented by V_{o1} and V_{o2} and they operate simultaneously in the synchronous Buck-WPT model.

$$I_m = I_{Lp} + \left(I_{Ls} * \frac{N_2}{N_1}\right) \quad (1)$$

The wired power output rail is identical to the traditional buck converter. The inductor L_p and the output capacitor C_{o1} have been utilized to develop the low-pass LC filter that delivers V_{o1} . There is no separate primary side control circuitry along with primary inductive coil on the power rail to the secondary coil. Rather, power stage of the buck is employed like a transmitter circuit as well as the primary inductor $L_p$as transmitting coil. For attaining wireless power transfer, the oscillation part of the primary inductor magnetizing current (I_m) is being utilized. It is due to the AC component of the magnetizing current produces alternating magnetic flux in the primary inductive coil (L_p), which is ideal to be used with an inductive wireless power transfer to secondary side receiver.

If a flat secondary inductive coil having inductance L_s is located close to the primary coil, then both of the coils are linked by a mutual inductance M. Due to this, some amount of power can indeed be transferred to the secondary receiver side. Compared with the traditional wireless topology, this system eradicates the separate transmitter side power circuits and transmitting coil, which minimizes the sizing, costs and control complexity of the overall structure.

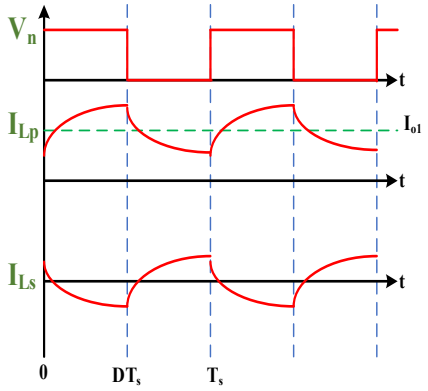

Fig. 2. Primary Operating Waveform of Single-Phase Isolated Buck system

III. RESULT AND DISCUSSION

Once the input and output specifications are identified, the next step is to choose a suitably coupled inductor by calculating the turns ratio required to produce the intended secondary voltage output. The specifications for the robust isolated buck converter system is shown in table I.

TABLE I. SYSTEM SPECIFICATIONS

Parameter	*Description*	*Value*
V_{IN}	Input Voltage	15-40V
V_{O1}	Buck Output Voltage	10V
I_{O1}	Buck Output Current	5A
V_{O2}	Secondary Load Voltage	5V
I_{O2}	Secondary Load Current	1.5A
f_{sw}	Switching Frequency	200Khz
k	Coefficient of Coupling	0.95
V_f	Rectifier Forward Voltage Drop	2V

A. THEORETICAL ANALYSIS

The designed approach is merely a standard buck power converter with power inductor substituted by a coupled inductor and thus having an isolated secondary side. The primary side output is still controlled in the same way that a

standard dc-dc buck converter is, and thus the suitable transfer function from supply side to buck load output is:

$$V_{o1} = D * V_{in} \quad (2)$$

To create the two electrical output track, two coils would be required. The coupled inductor's secondary coil serves as the power input for the isolated load, which is comprised of a full bridge diode rectifier and a filter capacitor in its most basic type. To enhance the performance of the secondary load, the full bridge diode rectifier is used with a filter capacitor, so that they work together to provide a DC regulated load voltage to the secondary side. Using Kirchhoff's voltage law (KVL) through the secondary circuit, we can determine the secondary output voltage as:

$$V_{o2} = \left(V_{o1} * \frac{N_2}{N_1}\right) - V_f \quad (3)$$

During the ON-time, high-side MOSFET is turned on and appears to be a short circuit. This implies that the SW node voltage is same as the source voltage, and the voltage across the primary coil is:

$$V_{Lp} = (V_{in} - V_{o1}) \quad (4)$$

As this is a buck topology ($V_{in} > V_{o1}$), so V_{Lp} is positive when MOSFET is on. The secondary voltage induced across the secondary coil is calculated as below:

$$V_{Ls} = \left(V_{Lp} * \frac{N_2}{N_1}\right) \quad (5)$$

Seeing as current reaches the dotted terminal of the primary coil, the voltage at the dotted terminal of the secondary coil is positive, according to the dot convention. It implies that the diode rectifier is reverse biased with regard to the isolated ground, and the filter capacitor powers to the load. When main Mosfet is turned on, the voltage developed across the rectifier is 2 $V_{D,max}$

where,

$$V_{D,max} = V_{o2} + \left(\frac{N_2}{N_1}\right)(V_{in} - V_{o1}) \quad (6)$$

The high side MOSFET node voltage is taken down to GND potential in the off time, as the low-side MOSFET is turned on. Now the voltage developed across main winding is:

$$V_{Lp} = -V_{o1} \quad (7)$$

Following the exact method as during the turn on time, the voltage developed is now negative at the dotted terminal of the secondary coil, resulting in the diodes of the rectifier being conducting state. The secondary coil now serves as a current source, transmitting energy from the main side to the load of isolated side. The DC part of the secondary current is fed to the load in the exact manner as in typical buck mode, and the oscillating part of the current energies the filter capacitor.

The magnetizing current waveform is similar to the prevalent triangular inductor current waveform observed in normal buck operation. This magnetizing current of mutual inductor and the average both side currents are calculated as given in (8)-(10):

$$I_m = I_{Lp} + \left(I_{Ls} * \frac{N_2}{N_1}\right) \quad (8)$$

$$I_{o1} = I_{Lp} \quad (9)$$

$$I_{o2} = I_{Ls} \quad (10)$$

the peak-to-peak current ripple of the magnetizing current waveform, is determined as below:

$$\Delta I_m = \frac{(V_{in} - V_{o1})t_{on}}{L_p} \quad (11)$$

Now, the maximum primary coil current is calculated as,

$$I_{Lp,Peak} = I_{o1} + \left(\frac{N_2}{N_1} * I_{o2}\right) + \frac{\Delta I_m}{2} \quad (12)$$

and the inductance of the main coil is determined using the normal buck operation as,

$$L_p = V_{Lp} * \frac{\Delta t}{\Delta I_{Lp}} \quad (13)$$

Where ΔI_{Lp} term denotes the peak-to-peak current ripple, ΔI_m and is typically 30% to 40% of the magnetizing current delivered by the converter.

The peak-to-peak magnetizing current ripple (ΔI_m) can be modified to the larger or lesser value based on the user's requirements. The chosen ΔI_m is valid until the primary winding current does not exceed either the high-side or negative current limits. Due to above, the derived primary inductor (L_p) is not a standard inductance value, hence a 10-µH inductor is preferred.

The duty ratio and leakage inductance are also important considerations in the working of this system. Actual transformers and paired inductors have certain leakage inductance due to magnetic flux which is not a part of both windings. This leakage flux brings down secondary side wattage by reducing the rate at which the secondary side current can ramp up. For cases of higher leakage inductance, the ramp rate of the current in the secondary side is reduced compared to that of a lower leakage case. This indicates that it requires more time for the same energy input to be transmitted from primary to secondary.

For a set frequency aspect, this involves selecting a lesser highest duty ratio to make sure that there is adequate off-time for energy to be transmitted from primary to secondary. By convention, the upper limit of duty ratio in this topology is set at 50%; higher duty ratio leads to lesser off-time of the switch, which results in greater negative maximum currents getting reflected to the primary coil. Leakage inductance should thus be kept to a minimum to confirm the widest duty cycle range.

As a result, the µH coupled inductor chosen is sufficient to maintain that the maximum current boundaries are not exceeded. This inductor should also have a saturation current rating that is at least comparable to the device's peak short circuit current limit. The peak short circuit current limit is used in this scenario to make sure that the threshold is not surpassed under worst-case scenarios, just like explained previously.

The level of output voltage ripple and load dynamic response that the standard buck converter may attain on its

main load side is governed by the output filter capacitor and it is calculated as:

$$C_{o1} = \frac{\Delta I_{o1}}{f_{sw} * \Delta V_{o1} * K}\left[(1-D)(1+P) + \frac{K^2}{12}(2-P)\right] \quad (14)$$

Where,
ΔVo1 = output voltage ripple
ΔIo1 = output current transient
P = ripple component

During the converter's on-time, the secondary output capacitor must be capable of delivering the secondary demand. Equation (16)-(17) calculate the secondary coil inductance and output filter capacitance as below:

$$L_s = L_p * \left(\frac{N_2}{N_1}\right)^2 \quad (15)$$

$$C_{o2} = \frac{I_{o2} * D_{max}}{f_{sw} * \Delta V_{o2}} \quad (16)$$

The input voltage (V_{in}) , the input current (I_{in}) , the high side MOSFET voltage (V_{sw1}) , the primary output voltage (V_{o2}), the primary output current (I_{o1}), the secondary output voltage (V_{o2}) , the secondary output current (I_{o2}) and the current through the primary and secondary winding (I_{Lp} & I_{Ls}) are all shown in the steady state waveforms below. Because the secondary filter capacitor must provide the current to the secondary load during the device's on-time, this is the severe instance of secondary load voltage ripple.

B. Simulation

To validate the viability of the proposed isolated buck system, a buck converter employing coupled inductor is simulated by using MATLAB/SIMULINK. The details of the simulated system parameters are shown in TABLE I.

Fig. 3 represents the steady state simulated waveforms of primary and secondary coil current (I_{Lp}& I_{Ls}). The figure shows that primary and secondary coil currents are 180° out of phase as this is required to transfer the power from primary to secondary side. This simulation result is consistent with the theoretical analysis. Fig. 4-5 represents the steady state simulated waveforms of normal buck load voltage and load current (V_{o1}& I_{o1}) and secondary side load voltage and current waveforms (V_{o2}& I_{o2}) at nominal input dc voltage of 20 volts and duty cycle of 50%. These waveforms show that the load voltages and load currents are ripple free. Fig. 6 represents the steady state waveforms of the system input voltage and current (V_{in}& I_{in}). All of the aforementioned simulated findings match with the theoretical study done in section II A.

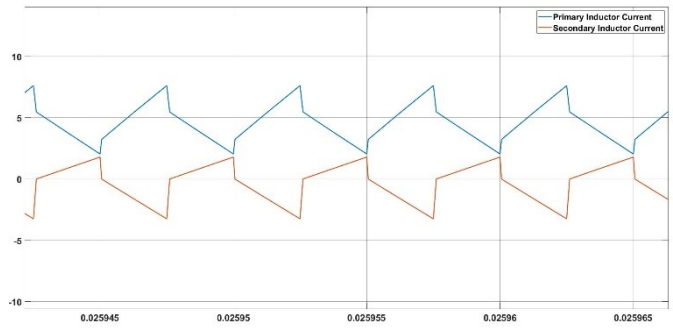

Fig. 3. Primary *and Secondary Inductor Current Waveforms*

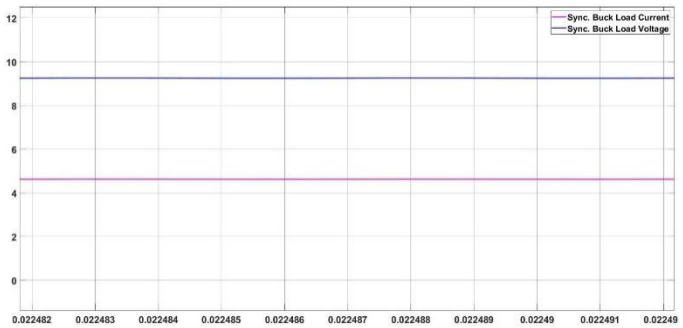

Fig. 4. Buck Load Voltage and Load Current Waveforms at V_{IN}=20Volts

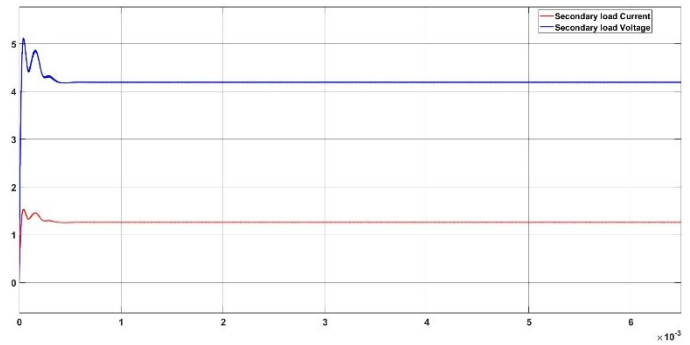

Fig. 5. *Secondary side Load Voltage and Current Waveforms at V_{IN}=20Volts*

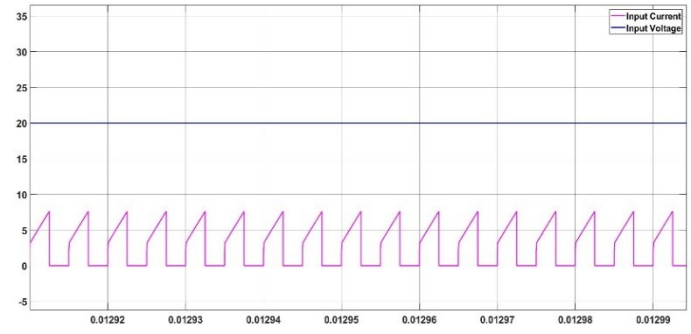

Fig. 6. *System input Voltage and Current Waveforms*

IV. Conclusion

A new isolated buck converter based on coupled inductor is proposed in this paper to generate an isolated secondary output along with normal wired buck output. To provide isolated output, this system facilitates compact, economical, and lesser number of required parameters. And the overall system cost, complexity and size can be efficiently restricted, especially for the case of using the secondary load to act as regulated power supply to the main Mosfet of the system. The secondary side is carefully designed so that it must supply required gate voltage and average charge to properly turn on the main Mosfet. The proposal method has been effectively verified with theoretical analysis and simulation results, and is hopefully applied to the main Mosfet of the system without the requirement of a regulated power supply. In this simulated circuit design, two resistive loads are used. We will implement this methodology in our future work in the experimental prototype and buck resistive load will be replaced by the battery load.

References

[1] Qi Cheng, Liuyan Chen and J. Guo, "A fully integrated AC-DC regulator over wide frequency range for implantable bio-medical devices," 2014 International SoC Design Conference (ISOCC), 2014, pp. 44-45, doi: 10.1109/ISOCC.2014.7087586

[2] J. H. Cha, W. Park and M. Je, "A CMOS Rectifier with a Cross-Coupled Latched Comparator for Wireless Power Transfer in Biomedical Applications," in IEEE Transactions on Circuits and Systems II: Express Briefs, vol. 59, no. 7, pp. 409-413, July 2012, doi: 10.1109/TCSII.2012.2198977.

[3] H. -M. Lee and M. Ghovanloo, "An Integrated Power-Efficient Active Rectifier with Offset-Controlled High-Speed Comparators for Inductively Powered Applications," in IEEE Transactions on Circuits and Systems I: Regular Papers, vol. 58, no. 8, pp. 1749-1760, Aug. 2011, doi: 10.1109/TCSI.2010.2103172.

[4] R. Singh, M. K. Patel and J. Dhar, "Efficient Secondary Power Conversion Techniques in Multi-output DC-DC Converters," 2020 IEEE First International Conference on Smart Technologies for Power, Energy and Control (STPEC), 2020, pp. 1-4, doi: 10.1109/STPEC49749.2020.9297792.

[5] Xu Peng, Yuan-Chen Ren, Ye Mao and F. C. Lee, "A family of novel interleaved DC/DC converters for low-voltage high-current voltage regulator module applications," 2001 IEEE 32nd Annual Power Electronics Specialists Conference (IEEE Cat. No.01CH37230), 2001, pp. 1507-1511 vol. 3, doi: 10.1109/PESC.2001.954332.

[6] Brown, M.C., 2012. Practical switching power supply design. Elsevier.

[7] Maksimovic, D., and Erickson, R.W. Fundamentals of Power Electronics. Springer, 2004.

[8] Hurley, W.G., and Wölfle, W.H. Transformers and Inductors for Power Electronics: Theory, Design and Applications. John Wiley & Sons, 2013.

[9] Zhang, Z., Ngo, K.D. and Nilles, J.L., 2014, March. A 30-W flyback converter operating at 5 MHz. In 2014 IEEE Applied Power Electronics Conference and Exposition-APEC 2014 (pp. 1415-1421). IEEE.

[10] Sullivan, C.R., Abdallah, T., and Fujiwara, T. "Optimization of a Flyback Transformer Winding Considering Two-Dimensional Field Effects, Cost and Loss." APEC 2001 Sixteenth Annual IEEE Applied Power Electronics Conference and Exposition (2001) 116-122.

[11] W. Huang, J. A. Abu Qahouq, and Z. Dang. "CCM-DCM Power-Multiplexed Control Scheme for Single-Inductor Multiple-Output DC-DC Power Converter with No Cross-Regulation," IEEE Trans. Ind. Applications, vol. PP, issue 99, pp. 1-1, 2016.

[12] Wangxin Huang and Jaber Abu Qahouq, "Input-Voltage Ripple-Based Sensorless current sharing auto-tuning controller for multiphase DC-DC converters," IEEE Transactions on Industry Applications, Vol. 52, No. 5, Page(s): 4117-4125, Sept.-Oct, 2016.

[13] Z. Dang and J. A. Abu Qahouq, "Permanent magnet coupled power inductor for multi-phase DC-DC power converters," IEEE Trans. Ind. Electron., vol. 99, pp. 1-1, 2016.

[14] Bertoluzzo M, Giacomuzzi S, Kumar A. Design of a Bidirectional Wireless Power Transfer System for Vehicle-to-Home Applications. Vehicles. 2021; 3(3):406-425.

[15] Abhay Kumar, N. Neogi , "Bidirectional Converter And Energy Storage System" published in International Journal of Enhanced Research in Science Technology & Engineering, Vol 4 Issue 6, June-2015, pp: (15-23